Efficient Analysis of Harmonic Losses in PWM Voltage Source Induction Machine Drives with Modelica

Johannes V. Gragger Anton Haumer Christian Kral Franz Pirker
Arsenal Research
Giefinggasse 2, 1210 Vienna, Austria

Abstract

This paper presents an approach to calculate the copper and core losses caused by harmonics of the PWM of a voltage source inverter. For the analysis some models of the *Smart Electric Drives* (SED) library, and additionally, a *Modelica* library for modeling AC circuits by means of electric time phasors, are used. With the proposed analysis the influence of space phasor PWM signals on the machine efficiency is investigated. A *Modelica* model of a speed controlled induction machine drive working at different load points and different switching frequencies is presented. The results of the simulation are compared and discussed.

Keywords: induction machine, inverter, speed controlled drive, efficiency, copper losses, core losses, space phasor PWM, SED library

1 Introduction

In most variable speed drives pulse width modulation (PWM) voltage source inverters are used. Usually machine design tools only consider the fundamental harmonic of the stator voltage when calculating the losses. The major aim of the presented work is to investigate the negative impact of PWM switching on additional losses in the machine windings and the iron cores. These additional losses are caused by harmonics of the voltage and the current due to the PWM. The harmonic losses of the induction machine are modeled using the AC library, which is based on the stationary analysis with complex time phasors [1].

A number of algorithms for PWM voltage generation are available. Some well known techniques are unipolar voltage switching and bipolar voltage switching [2], harmonic elimination [3] and space vector PWM [4]. In fact there are many more techniques in which the basic principles of the ones mentioned are used with some modifications. Different PWM algorithms cause different voltage harmonics. These voltage harmonics give rise to current harmonics due to the machine impedance. The voltage harmonics cause additional core losses whereas the current harmonics cause additional losses in the stator and rotor winding of the machine. Moreover, the frequency of the carrier signal has a significant influence on the voltage and current spectra and consequently increases the losses arising in the machine. It is widely accepted that PWM switching has a negative impact on the efficiency of the drive and some efforts had been undergone to calculate the amount of losses caused by PWM switching.

In [5, 6, 7, 8, 9] finite element analysis (FEA) techniques are implemented, which require high computational expenses for calculating the additional losses. In an FEA model the ohmic heat losses due to the PWM switching are inherently covered. The additional core losses are computed by a frequency and flux dependent model, which is evaluated locally throughout the machine volume.

Alternatively, the harmonic losses can be assessed keeping the processing efforts low by defining specific loss factors [10]. In this case it is crucial to keep the energy balance between the electric terminals and the shaft of the machine consistent.

In this paper the energy balance is implemented straight forward by defining an equivalent circuit [11, 12, 13, 14]. The presented work is based solely on analytical equations using data from conventional induction machine calculation programs without FEA. An equivalent circuit with elements taking deep bar effects and the influence of the stator voltage and the stator frequency on iron losses into account is used to calculate the harmonic losses with the principle of superposition. The proposed models are designed such way that it takes only little effort to replace the PWM algorithm by an alternative one and to change machine

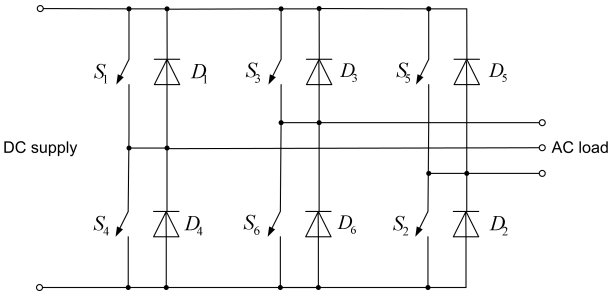

Figure 1: Three phase full bridge.

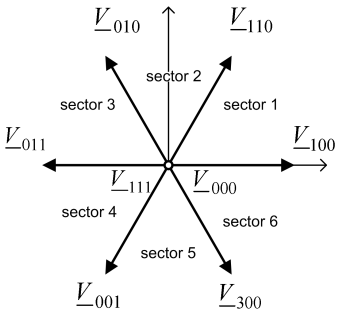

Figure 2: Possible voltage space vectors of a three phase space vector PWM.

data in order to benchmark different variable speed drive setups.

2 PWM voltage generation

The PWM waveform depends on the control unit and the converter topology. In this work one of the most commonly used PWM waveforms is analyzed, the space vector PWM. Space vector PWM can be implemented if a three phase converter of the topology shown in fig. 1 is used. The states of the six switches (S_1 to S_6) must be chosen such way that the switches of one leg of the converter switch complementary. Neglecting dead times, it must hold that whenever one switch of a leg is ON the other one must be OFF. By no means both can be ON at the same time.

There are eight possible combinations for the switch commands, which result in seven elementary output voltage space vectors as shown in fig. 2. By using PWM for switching between these seven elementary space vectors any space vector position can be realized. The output phase voltages of a space phasor PWM controlled three phase full bridge are shown in fig. 3. Using the models of ideal switching converters and the respective PWM control blocks from the SED library [15, 16], it is possible to compare the "quality" of PWM signals with different switching frequencies (and with different switching algorithms). In fig. 4 the spectra of space vector PWM with two different frequency ratios are shown where v_{ref} is the phase voltage amplitude of the reference space vector rotating with constant angular speed and magnitude and f_{ref} is the frequency of the phase voltage. The frequency per unit (p.u.) is $\frac{f}{f_{ref}}$ and the voltage p.u. is $\frac{v}{v_{ref}}$. It appears that space vector PWM with high switching frequency, f_{Switch}, causes considerably lower harmonics with low order numbers than space vector PWM with low switching frequency. If the spectrum of the PWM voltage signal and the frequency dependent impedances of the machine are known the harmonic copper losses and the harmonic core losses can be calculated. It can be shown that high switching frequencies help decreasing the iron losses and the copper losses in voltage source inverter drives.

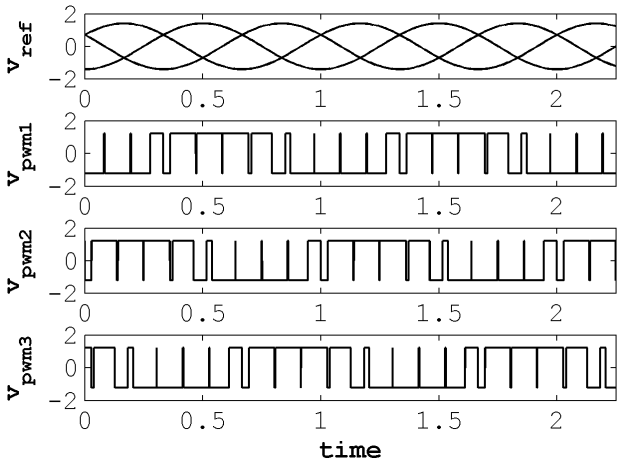

Figure 3: Reference signals and resulting PWM signals, v_{PWM}, of the investigated space vector PWM algorithm.

3 Model of the copper losses

The copper losses in an induction machine can be determined by using the well known single phase equivalent circuit [17]. Figure 5 shows the *Modelica* model of the investigated induction machine. This equivalent circuit represents the machine behavior in steady state operation. The connectors used in the equivalent circuit model contain complex current time phasors as flow variables and complex voltage time phasors as potential variables. Furthermore, the reference frame of the time phasors is defined by a reference angle φ in the connectors. For the calculation of the copper losses the deep bar effects of the rotor stray inductance and

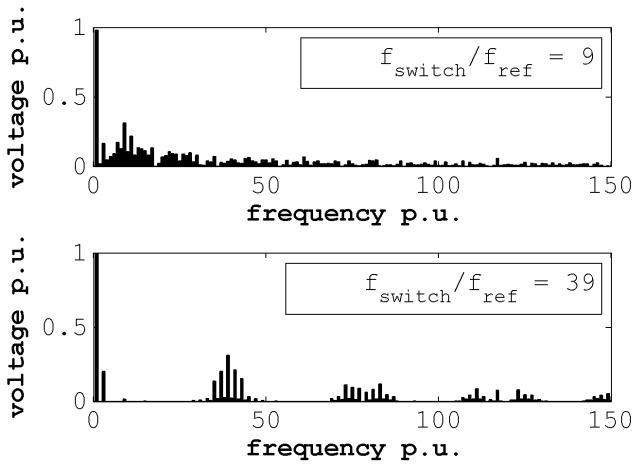

Figure 4: Spectra of space vector PWM voltages with low and with high switching frequency.

the rotor resistance are considered. Skin effects in the stator resistance and stator inductance are neglected because they can be mostly avoided through wires with small radial length in the stator winding [18]. Saturation effects are neglected as well.

The slip with respect to a certain harmonic depends on the orders of this harmonic. It can be shown that the rotational directions of the spatial harmonic waves of the stator field are dependent on the order number [19]. Therefore the slip related to the different voltage harmonics,

$$s_\nu = \frac{\omega_\nu - \omega_m}{\omega_\nu} \tag{1}$$

where ω_m is the shaft speed of an equivalent two pole machine and the angular velocities of the harmonic waves of the stator quantities,

$$\omega_\nu = \omega_1 \cdot \nu. \tag{2}$$

Using (1) and (2) the slip can be written as

$$s_\nu = 1 - \frac{1 - s_1}{\nu}. \tag{3}$$

In a symmetric induction machine with m phases fed by PWM voltages the order numbers of the harmonics of the stator field [20] are

$$\nu = 2 \cdot m \cdot k + 1, \tag{4}$$

where

$$k = \{0, \pm 1, \pm 2, \pm 3, \ldots\}. \tag{5}$$

It is well known that

$$R'_{r\nu} = \frac{R_{r\nu}}{s_\nu} = R_{r\nu} + R_{mech\nu} \tag{6}$$

with

$$R_{mech\nu} = R_{r\nu} \frac{1 - s_\nu}{s_\nu}. \tag{7}$$

For each harmonic order, the power dissipated by $R_{r\nu}$ represents the copper losses in the rotor and the power dissipated by $R_{mech\nu}$ represents the mechanical power of the machine distributed to the shaft (without considering stray load losses) [17].

According to [21] the deep bar effects in rotor bars with rectangular profile can be considered by a resistance factor

$$K_{R\nu} = \xi_\nu \cdot \frac{\sinh(2\xi_\nu) + \sin(2\xi_\nu)}{\cosh(2\xi_\nu) - \cos(2\xi_\nu)} \tag{8}$$

and an inductance factor

$$K_{I\nu} = \frac{3}{2\xi_\nu} \cdot \frac{\sinh(2\xi_\nu) - \sin(2\xi_\nu)}{\cosh(2\xi_\nu) - \cos(2\xi_\nu)}, \tag{9}$$

with

$$\xi_\nu = h \cdot \sqrt{\frac{\mu_0 \cdot 2\pi f_\nu}{2\rho} \cdot \frac{b}{b_s}}. \tag{10}$$

The subsidiary quantity ξ_ν is a function of the bar height, h, the frequency of the voltage harmonic, f_ν, the specific resistance of the rotor bars, ρ, the width of the rotor bar, b, and the width of the rotor slot, b_s. Hence, the rotor resistance,

$$R'_{r\nu} = K_{R\nu} \cdot R'_{r,var} + R'_{r,const}. \tag{11}$$

In (11) the constant resistance, $R'_{r,const}$, represents the end rings and the parts of the rotor bars that are not embedded in the slots whereas the variable resistance, $K_{R\nu} \cdot R'_{r,var}$, represents the parts of the rotor bars that are embedded in the slot.

The rotor stray inductance is modeled the same way:

$$L'_{r\sigma\nu} = K_{I\nu} \cdot L'_{r\sigma,var} + L'_{r\sigma,const} \tag{12}$$

By calculating the stator current, $\underline{I}_{s\nu}$, and the rotor current, $\underline{I}_{r\nu}$, of the single phase equivalent circuit for all harmonics, the stator and rotor copper loss increase due to the harmonics can be expressed by

$$p_{Cu,s\Sigma\nu} = \frac{\Sigma(|\underline{I}_{s\nu}|^2)}{|\underline{I}_{s1}|^2} - 1 \tag{13}$$

and

$$p_{Cu,r\Sigma\nu} = \frac{\Sigma(R_{r\nu} \cdot |\underline{I}'_{r\nu}|^2)}{R_{r1} \cdot |\underline{I}'_{r1}|^2} - 1 \tag{14}$$

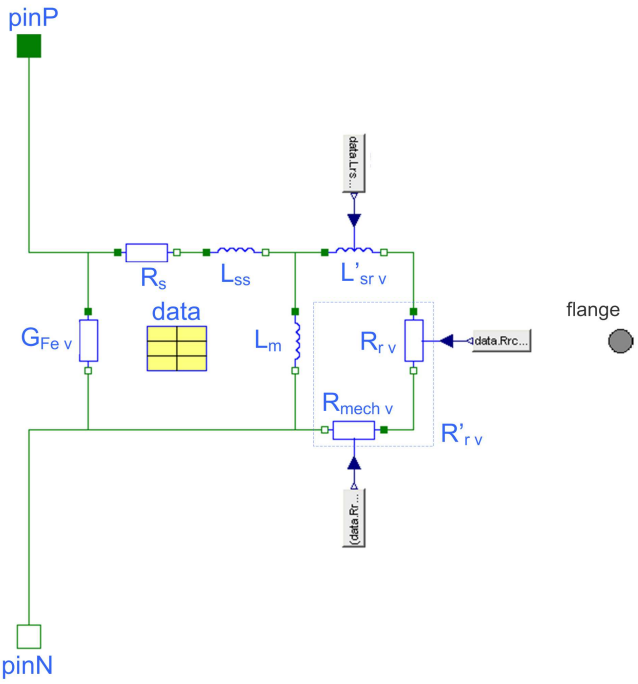

Figure 5: Equivalent circuit of an induction machine implemented with *Modelica*.

Consequently, the total harmonic copper losses are

$$P_{Cu\sum\nu} = P_{Cu,s1} \cdot p_{Cu,s\sum\nu} + P_{Cu,r1} \cdot p_{Cu,r\sum\nu} \tag{15}$$

where $P_{Cu,s1}$ and $P_{Cu,r1}$ are the stator and rotor copper losses with respect to the fundamental wave.

4 Model of the core losses

The core losses, P_{Fe}, in an induction machine can be divided into two parts: the hysteresis losses and the eddy current losses [22, 23, 24, 25]. Hysteresis losses, $P_{Fe,h}$, and eddy current losses, $P_{Fe,e}$, can both be expressed as functions of the magnetic flux linkage, ψ, and the stator frequency, f:

$$P_{Fe,h} = F_h\{\psi^2, f\} \tag{16}$$

$$P_{Fe,e} = F_e\{\psi^2, f^2\}. \tag{17}$$

Considering that the voltage is directly proportional to the flux linkage and the frequency according to

$$V_\nu = \psi_\nu \cdot \omega_\nu \tag{18}$$

the hysteresis losses and eddy current losses caused by the harmonics of the stator voltage can be calculated per unit to

$$p_{Fe,h\nu} = [(\frac{f_1 \cdot V_{s\nu}}{f_\nu \cdot V_{s1}})^2 \cdot \frac{f_\nu}{f_1}] = \frac{f_1 \cdot V_{s\nu}^2}{f_\nu \cdot V_{s1}^2} \tag{19}$$

$$p_{Fe,e\nu} = [(\frac{f_1 \cdot V_{s\nu}}{f_\nu \cdot V_{s1}})^2 \cdot (\frac{f_\nu}{f_1})^2] = \frac{V_{s\nu}^2}{V_{s1}^2}. \tag{20}$$

In the equivalent circuit shown in fig. 5 the hysteresis and the eddy current losses are both considered in one conductor $G_{Fe\nu}$. Using the hysteresis losses, $P_{Fe,h1}$, and the eddy current losses, $P_{Fe,e1}$, of the fundamental together with (19) and (20),

$$G_{Fe\nu} = \frac{P_{Fe,h1}}{3 \cdot V_{s\nu}^2} \cdot p_{Fe,h\nu} + \frac{P_{Fe,e1}}{3 \cdot V_{s\nu}^2} \cdot p_{Fe,e\nu}. \tag{21}$$

Hence, the total harmonic core losses

$$P_{Fe\sum\nu} = 3 \cdot \sum(G_{Fe\nu} \cdot V_{s\nu}^2) \tag{22}$$

which can also be written as

$$\begin{aligned} P_{Fe\sum\nu} &= P_{Fe,h1} \cdot \{[\sum p_{Fe,h\nu}] - 1\} + \\ &+ P_{Fe,e1} \cdot \{[\sum p_{Fe,e\nu}] - 1\}. \end{aligned} \tag{23}$$

5 Simulation setup

In mining, chemical, waste water, gas or oil industries there are high-power medium-voltage variable speed drives used that work with IGCT or IGBT converters. Such IGCT converters have switching frequency ranges around 1 kHz and IGBT converters work with frequencies up to 10 kHz [26].

In this paper a high-power medium-voltage water pump drive is simulated. The specifications of the investigated induction machine are shown in table 1. The spectra of the voltage waveforms generated by space vector PWM are calculated using the SED library and the *Modelica* Standard library in a Dymola simulation environment. In fig. 6 the model calculating the harmonic components from the inverter voltage is shown. The model contains three ideal reference voltage signals, a block generating the PWM switching commands, and a model representing a three phase full bridge with integrated DC-link voltage source as well as a Fourier analysis block. In the Fourier analysis block the Fourier coefficients, a_k and b_k, get calculated according to the Euler-Fourier formulas [27] with two integrators and a sine and a cosine signal source. The spectral components are computed by converting the Cartesian coordinates, a_k and b_k, to polar coordinates, d_k and φ_k. From the generated spectral components the harmonic losses are processed through a

Table 1: Parameters of the high-power medium-voltage induction machine.

Induction Machine		
Pole Pairs		2
Nominal Power	[kW]	1600
Nominal Frequency	[Hz]	50
Nominal Voltage	[V]	6000
Nominal PF		0.873
Nominal Slip	[%]	0.25

Fourier synthesis in the model shown in fig. 7. The encapsulated induction machine model applied for loss calculation is depicted in fig. 5. It is fed with an array of stator voltage time phasors.
In the induction machine model the inner torque components, $T_{innerν}$, with respect to a harmonic, ν, are computed by

$$T_{innerν} = p \cdot \frac{P_{inputν} - (P_{Cu,sν} + P_{Feν})}{(2 \cdot \pi \cdot f_ν)}, \qquad (24)$$

where p is the number of pole pairs, $P_{inputν}$ are the electrical input power components of the machine, $P_{Cu,sν}$ are the stator copper loss components, $P_{Feν}$ are the iron loss components, and $f_ν$ are the harmonic stator frequencies. The shaft speed of the induction machine is controlled by an integral action controller such way that the fundamental component of the mechanical power

$$P_{airgap1} = T_{inner1} \cdot (2 \cdot \pi \cdot f_1), \qquad (25)$$

matches the reference power, P_{ref}. Since the friction losses, P_{fr}, are not considered in the equivalent circuit, the reference power with respect to the shaft of the machine model is determined by

$$P_{ref} = P_{m,ref} + P_{fr}, \qquad (26)$$

where $P_{m,ref}$ is the desired mechanical power of the induction machine. If the actual power, P_{real}, at the shaft of the machine model matches P_{ref}, the desired operation point is reached.
The harmonic losses of the inverter drive are computed for two different operation points of the machine. In case A the machine is operated at nominal supply frequency, $f_{Nominal}$, and nominal mechanical power, $P_{Nominal}$. In case B the machine is simulated at $\frac{f_{Nominal}}{3}$ and $\frac{P_{Nominal}}{27}$. The reason for assessing case B is to investigate the influence of the harmonic losses specifically in variable speed drives that are connected

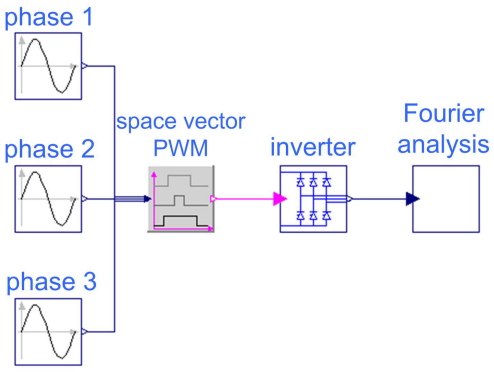

Figure 6: Model used for the PWM signal analysis.

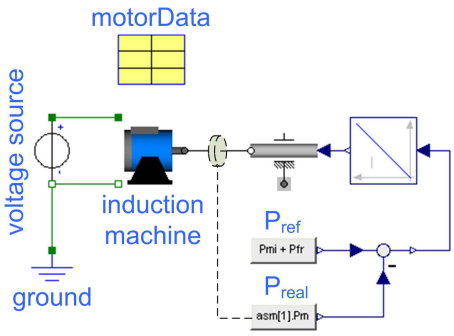

Figure 7: Model of the PWM voltage source induction machine drive.

with mechanical loads such as pumps or fans. Many of these loads have an approximately quadratic speed dependent load torque characteristic.
Besides the variation of the operation point also the converter switching frequency is varied. The harmonic spectra of the PWM voltages with switching frequencies of 1950 Hz, 1050 Hz and 450 Hz are calculated and fed to the machine model.

6 Simulation Results

In table 2 the simulation results of the machine fed with space vector PWM are presented. The investigations show that increasing the PWM switching frequency decreases the total harmonic core losses. The total harmonic core losses at a switching frequency of 450 Hz are about 60% higher than at a switching frequency of 1950 Hz. It can also be seen that the total harmonic copper losses rise much more than the total harmonic core losses. In case A, for instance, the total harmonic copper losses become more than ten times higher if the switching frequency gets decreased from

Table 2: Modelica simulation results of the high-power medium-voltage induction machine drive.

		Case A: $f = f_{Nominal}$ $P = P_{Nominal}$	Case B: $f = \frac{f_{Nominal}}{3}$ $P = \frac{P_{Nominal}}{27}$
Switching Frequency = 1950 Hz			
Machine Output Power (Fundamental)	[W]	1600000.00	59259.30
Shaft Speed	[rpm]	1496.34	499.62
Stator Current (Fundamental)	[A]	179.85	49.19
Power Factor (Fundamental)		0.87	0.38
Friction Losses	[W]	5566.00	1996.00
Core Losses (Fundamental)	[W]	10706.50	3039.31
Stator Copper Losses (Fundamental)	[W]	8453.70	630.36
Rotor Copper Losses (Fundamental)	[W]	3928.22	47.19
Core Losses (Harmonics)	[W]	582.59	377.65
Stator Copper Losses (Harmonics)	[W]	20.84	5.46
Rotor Copper Losses (Harmonics)	[W]	436.41	152.45
Efficiency (Fundamental)	**[%]**	**98.24**	**91.21**
Efficiency considering Harmonics	**[%]**	**98.18**	**90.46**
Switching Frequency = 1050 Hz			
Machine Output Power (Fundamental)	[W]	1600000.00	59259.30
Shaft Speed	[rpm]	1496.32	499.62
Stator Current (Fundamental)	[A]	180.33	49.18
Power Factor (Fundamental)		0.87	0.38
Friction Losses	[W]	5566.00	1996.00
Core Losses (Fundamental)	[W]	10651.60	3037.93
Stator Copper Losses (Fundamental)	[W]	8499.40	630.16
Rotor Copper Losses (Fundamental)	[W]	3952.34	47.21
Core Losses (Harmonics)	[W]	678.37	561.57
Stator Copper Losses (Harmonics)	[W]	73.31	21.81
Rotor Copper Losses (Harmonics)	[W]	1115.07	463.48
Efficiency (Fundamental)	**[%]**	**98.24**	**91.21**
Efficiency considering Harmonics	**[%]**	**98.13**	**89.76**
Switching Frequency = 450 Hz			
Machine Output Power (Fundamental)	[W]	1600000.00	59259.30
Shaft Speed	[rpm]	1496.17	499.61
Stator Current (Fundamental)	[A]	183.42	49.14
Power Factor (Fundamental)		0.87	0.38
Friction Losses	[W]	5566.00	1996.00
Core Losses (Fundamental)	[W]	10312.80	3029.27
Stator Copper Losses (Fundamental)	[W]	8796.23	628.91
Rotor Copper Losses (Fundamental)	[W]	4108.64	47.35
Core Losses (Harmonics)	[W]	917.97	763.86
Stator Copper Losses (Harmonics)	[W]	461.05	125.53
Rotor Copper Losses (Harmonics)	[W]	4429.64	1780.97
Efficiency (Fundamental)	**[%]**	**98.23**	**91.22**
Efficiency considering Harmonics	**[%]**	**97.88**	**87.62**

1950 Hz to 450 Hz. The results also show that the harmonic stator copper losses only make up for a small share of the entire losses caused by the PWM harmonics. The biggest parts of the PWM harmonic losses are the harmonic rotor copper losses, especially when the drive is operated at low switching frequencies. The overall machine efficiency without stray load losses is also presented in table 2.

It appears that the consideration of harmonic losses only causes an efficiency decrease from 98.24 % to 98.18 % in case A with $f_{switch} = 1950$ Hz. The efficiency decreases from 98.23 % to 97.88 % for $f_{switch} = 450$ Hz. For case B the impact of the harmonics is much higher on the efficiency. At $f_{switch} = 1950$ Hz the efficiency decreases from 91.21 % to 90.46 %. The largest impact on the efficiency is due to a switching frequency $f_{switch} = 450$ Hz.

From this comparison one can conclude that when designing a machine for variable speed drives the PWM harmonic losses should be taken into account, especially if PWM frequencies below 1 kHz are used. Furthermore, the overall efficiency values show that as long as the machine is operated close to the nominal operation point (case A) with switching frequencies above 1 kHz the PWM harmonic losses can be neglected.

7 Conclusions

An analytical approach to calculate the copper and core losses caused by the harmonics of PWM voltages in variable speed induction machine drives is presented. The derived equations are implemented in *Modelica* language applying the AC library for modeling electric circuits by means of time phasors. By using the proposed models the PWM harmonic losses of a high-power medium-voltage induction machine with 1600 kW are calculated. Furthermore, the influence of reduced load and changes in the switching frequency are investigated. The results show that if the switching frequency is low and the machine is likely to be operated at low load points the PWM harmonic losses can decrease the overall efficiency of the machine considerably. Still, as long as the switching frequencies of the PWM are above 1 kHz and the load point does not vary significantly from the nominal load point the PWM harmonic losses can be neglected.

References

[1] A. Haumer, C. Kral, J. V. Gragger, and H. Kapeller, "Quasi-stationary modeling and simulation of electrical circuits using complex phasors", *International Modelica Conference, 6th, Bielefeld, Germany*, 2008.

[2] Mohan and Robbins, *Power Electronics*, J. Wiley Verlag, New York, 2 edition, 1989.

[3] H. S. Patel and R. G. Hoft, "Generalized techniques of harmonic elimination and voltage control in thyristor inverters: Part I-harmonic elimination", *IEEE Transactions on Industry Applications*, vol. IA-9, Issue 3, pp. 310–317, 1973.

[4] H.W. van der Broeck, H. C. Skudelny, and G.V. Stanke, "Analysis and realization of a pulsewidth modulator based on voltage space vectors", *IEEE Transactions on Industry Applications*, vol. 24, No. 1, pp. 142–150, 1988.

[5] T.C. Green, C.A. Hernandez-Aramburo, and A.C. Smith, "Losses in grid and inverter supplied induction machine drives", *IEE Proceedings - Electric Power Applications*, vol. 150, no. 6, pp. 712–724, 11 2003.

[6] Y. Wu, R.A. McMahon, Y. Zhan, and A.M. Knight, "Impact of PWM schemes on induction motor losses", *41st IAS Annual Meeting, IEEE Industry Applications Conference*, vol. 2, pp. 813–818, 8-12 Oct. 2006.

[7] C.A. Hernandez-Aramburo, T.C. Green, and S. Smith, "Assessment of power losses of an inverter-driven induction machine with its experimental validation", *IEEE Transactions on Industry Applications*, vol. 39, Issue 4, pp. 994–1004, 2003.

[8] S. Mukherjee, G.E. Adams, and R.G. Hoft, "FEM analysis of inverter-induction motor rotor conduction losses", *IEEE Transactions on Energy Conversion*, vol. 4, no. 4, pp. 671–680, Dec. 1989.

[9] A.M. Knight, P.D. Malliband, C.Y. Leong, and R.A. McMahon, "Power losses in small inverter-fed induction motors", *IEEE International Conference on Electric Machines and Drives*, pp. 601–607, 15-18 May 2005.

[10] A. Boglietti, G. Griva, M. Pastorelli, F. Profumo, and T. Adam, "Different PWM modulation techniques indexes performance evaluation", *IEEE International Symposium on Industrial Electronics, ISIE'93 - Budapest.*, pp. 193–199, 1993.

[11] V. Kinnares, S. Potivejkul, and B. Sawetsakulanond, "Modified harmonic loss model in PWM fed induction machines", *IEEE Asia-Pacific Conference on Circuits and Systems, IEEE APCCAS*, pp. 535–538, 24-27 Nov. 1998.

[12] Isao Takahashi and Hiroshi Mochikawa, "A new control of PWM inverter waveform for minimum loss operation of an induction motor drive", *IEEE Transactions on Industry Applications*, vol. 21, no. 3, pp. 580–587, May 1985.

[13] H.W. van der Broeck and H. Skudelny, "Analytical analysis of the harmonic effects of a pwm ac drive", *IEEE Transactions on Power Electronics*, vol. 3,2, pp. 216–223, 1988.

[14] E. N. Hildebrand and H. Roehrdanz, "Losses in three-phase induction machines fed by PWM converter", *IEEE Transactions on Energy Conversion*, vol. 16, no. 3, pp. 228–233, Sept. 2001.

[15] H. Giuliani, D. Simic, J. V. Gragger, C. Kral, and F. Pirker, "Optimization of a four wheel drive hybrid vehicle by means of the SmartElectricDrives and the SmartPowerTrains library", *The 22nd International Battery, Hybrid and Fuel Cell Electric Vehicle Symposium & Exposition, EVS22*, 2006.

[16] J.V. Gragger, H. Giuliani, C. Kral, T. Bäuml, H. Kapeller, and F. Pirker, "The SmartElectricDrives Library – powerful models for fast simulations of electric drives", *5th International Modelica Conference 2006, Vienna, Austria*, 2006.

[17] R. Fischer, *Elektrische Maschinen*, Carl Hanser, München, 9 edition, 1995.

[18] H. Sequenz, *Die Wicklungen elektrischer Maschinen*, vol. 3, Springer Verlag, Wien, 1954.

[19] G. Müller, *Elektrische Maschinen - Theorie rotierender elektrischer Maschinen*, VEB Verlag Technik, Berlin, 2 edition, 1967.

[20] H. Kleinrath, *Stromrichtergespeiste Drehfeldmaschinen*, Springer Verlag, Wien, 1980.

[21] W. Schuisky, *Berechnung elektrischer Maschinen*, Springer Verlag, Wien, 1960.

[22] Th. Bödenfeld and H. Sequenz, *Elektrische Maschinen*, Springer Verlag, Wien, 7 edition, 1965.

[23] G. Müller, *Elektrische Maschinen - Grundlagen, Aufbau und Wirkungsweise*, VEB Verlag Technik, Berlin, 4 edition, 1977.

[24] V. Del Toro, *Electric Machines and Power Systems*, Prentice-Hall, Englewood Cliffs, NJ, 1985.

[25] I. Boldea and A. Nasar, *The Induction Machine Handbook*, CRC Press, London, 2002.

[26] B. Bose, *Power Electronics and Motor Drives*, Elsevier, 2006.

[27] Bronstein and Semendjajew, *Taschenbuch der Mathematik*, B.G. Teubner Verlag, Leipzig, 19 edition, 1979.